Extreme events in multivariate deterministic systems

C. Nicolis*
Institut Royal Météorologique de Belgique 3 av. Circulaire, 1180 Brussels, Belgium

G. Nicolis
Interdisciplinary Center for Nonlinear Phenomena and Complex Systems Université Libre de Bruxelles, Campus Plaine, CP 231 bd du Triomphe, 1050 Brussels, Belgium

(Received 7 March 2012; published 29 May 2012)

The probabilistic properties of extreme values in multivariate deterministic dynamical systems are analyzed. It is shown that owing to the intertwining of unstable and stable modes the effect of dynamical complexity on the extremes tends to be masked, in the sense that the cumulative probability distribution of typical variables is differentiable and its associated probability density is continuous. Still, there exist combinations of variables probing the dominant unstable modes displaying singular behavior in the form of nondifferentiability of the cumulative distributions of extremes on certain sets of phase space points. Analytic evaluations and extensive numerical simulations are carried out for characteristic examples of Kolmogorov-type systems, for low-dimensional chaotic flows, and for spatially extended systems.

DOI: 10.1103/PhysRevE.85.056217 PACS number(s): 05.45.−a, 02.50.−r, 05.20.−y

I. INTRODUCTION

Extreme events are of great importance in a variety of contexts of relevance in both fundamental research and applications, from biological evolution to the breakdown of a mechanical structure, an earthquake, flooding, or a financial crisis. Ordinarily, in view of their unexpectedness and high variability they are considered to be governed by statistical laws. There exists a powerful statistical theory of extremes, which in its most familiar version stipulates that the successive values $x_0, \ldots, x_{n-1}$ of a representative variable x recorded at equally spaced times are independent identically distributed variables (i.i.d.r.v.'s), irrespectively of the number and nature of other variables that may actually be involved in the system of interest. In the asymptotic limit of infinite observational window this leads, under suitable linear scaling, to a universal generalized extreme value distribution (GEV) involving just three parameters [1].

On the other hand, at a fundamental level of description natural systems obey to deterministic evolution laws. In many situations of interest these laws generate complex behaviors in, for instance, the form of spatiotemporal chaos which confer to the system nontrivial probabilistic properties such as ergodicity and mixing. This enables one to construct from first principles the main quantities of interest in extreme value theory and to compare with the predictions of the classical statistical approach.

In a series of papers the present authors and V. Balakrishnan analyzed from this standpoint the prototypical class of deterministic systems amenable to one-dimensional iterative mappings in the interval and giving rise to quasiperiodic or to chaotic behaviors [2,3]. They showed that dynamical complexity is reflected at the level of extreme value statistics by the nondifferentiability of the cumulative probabilities $F_n(x) = \text{Prob}(x_0 \leqslant x, \ldots, x_{n-1} \leqslant x)$ on a set of points corresponding to the unstable periodic orbits of the mapping, or in which different iterates of the mapping cross each other. As a corollary, the probability density of extremes $\rho_n(x) = dF_n(x)/dx$ is discontinuous and nonmonotonic. These behaviors are very different from the ones predicted by classical statistical theory, in which both $F_n(x)$ and $\rho_n(x)$ are smooth functions of x.

Typically, iterative mappings in the interval arise when monitoring the successive intersections of the phase space trajectory of a continuous-time dynamical system on a Poincaré surface of section. Their merit is to capture in a compact way the processes of expansion and reinjection, which constitute the principal ingredients behind the complexity of the dynamics. Now, real world systems are as a rule multivariate continuous-time dynamical systems. Furthermore, their evolution involves an intricate intertwining between local expansion and contraction stages [4]. The question thus arises whether the singular behavior seen in the contracted description afforded by the one-dimensional mappings generated by the above mechanisms subsists at the level of the extremes associated to the individual variables $\{x_i(t)\}$ of such systems or, rather, it is smoothed out by the process of averaging over all the remaining variables and the associated unstable and stable directions. To the observer the role of dynamical complexity in the extreme value statistics would then be blurred, and applicability of the classical statistical theory of extremes would at first sight appear to be legitimate. The objective of the present work is to investigate the effects arising from the presence of several coupled variables on extreme value properties.

The general formulation is presented in Sec. II. Sections III and IV deal, successively, with discrete and continuous-time low-dimensional dynamical systems. The case of spatially extended systems is considered in Sec. V, and the main conclusions are summarized in Sec. VI.

II. FORMULATION

Let $\mathbf{x} = \{x_1, \cdots, x_M\}$ be the state of a dynamical system at a given time. In the presence of deterministic evolution laws,

*Corresponding author: cnicolis@oma.be

the state $\mathbf{x}_t$ to which $\mathbf{x}$ will be transformed after a lapse of time t will be related to $\mathbf{x}$ by the relation

$$\mathbf{x_t} = \mathbf{\Phi^t}(\mathbf{x}), \tag{1a}$$

where $\mathbf{\Phi}^t$ is a one-valued (not necessarily invertible) function of $\mathbf{x}$. In a discrete-time system $\mathbf{\Phi}^t$ is determined by an iterative mapping $\mathbf{\Phi}$ relating the values of $\mathbf{x}_{n+1}$ at a time t_{n+1} to those of $\mathbf{x}_n$ at a previous time t_n,

$$\mathbf{x_{n+1}} = \mathbf{\Phi}(\mathbf{x_n}). \tag{1b}$$

As noted in the Introduction a typical example is provided by the successive intersection points of a phase space trajectory with a Poincaré surface of section. In a continuous-time system $\mathbf{\Phi}^t$ represents on the other hand the solution of a set of coupled first order differential equations for the x_i. If the variables $\{x_i\}$ are monitored at regularly spaced times, $t_1, t_2, \ldots, t_n$, with $t_n - t_{n-1} = \Delta t$, then $t = n\Delta t$, and in view of the semigroup property (1a) takes the form

$$\mathbf{x}_{t+\Delta t} = \mathbf{\Phi}^{\Delta t}(\mathbf{x_t}),$$

which one can write in a form similar to (1b),

$$\mathbf{x_{n+1}} = \mathbf{g}(\mathbf{x_n}). \tag{1c}$$

Let $\{a_i\}$, $\{b_i\}$, be the upper and lower bounds of the values of $\{x_i\}$ during their time evolution,

$$a_i \leqslant x_i \leqslant b_i, \quad 1 \leqslant i \leqslant M. \tag{2}$$

The (cumulative) multivariate probability that in a time sequence of length n generated by Eqs. (1b) or (1c) all subsequent values $x_{i,m}$ $(i = 1, \ldots, M;\ m = 0, \ldots, n-1)$ are less than or equal to a certain prescribed set of extreme values $\{u_i\} = u_1, \ldots, u_M$ is then

$$\begin{aligned} &F_n(u_1, \ldots, u_M) \\ &= \int_{a_1}^{u_1} \cdots \int_{a_M}^{u_M} dx_1 \cdots dx_M \rho(x_1, \ldots, x_M) \\ &\quad \times \prod_{m=1}^{n-1} \theta\left(u_1 - \Phi_1^{(m)}(\{x_i\})\right) \cdots \theta\left(u_M - \Phi_M^{(m)}(\{x_i\})\right), \end{aligned} \tag{3}$$

where the superscript (m) denotes the mth iterate, θ is the Heaviside step function, and ρ is the invariant probability. A similar relation holds if the mapping $\mathbf{\Phi}$ in (1b) is replaced by $\mathbf{g}$ in Eq. (1c).

In most situations of interest in connection with extreme events, the quantities one is actually monitoring experimentally are not the full set of x_i but, rather, a limited number of them or even more typically quantities $\{z_\alpha\}$ which are combinations of the x_i,

$$z_\alpha = f_\alpha(x_1, \ldots, x_M) \quad \alpha = 1, \ldots, A \quad (A \ll M). \tag{4}$$

It often happens (as, e.g., in hydrology, where the main z variable of interest is a river discharge) that the z are linear combinations of the x_i [5],

$$z = \sum_{i=1}^{M} \alpha_i x_i, \qquad \sum_{i=1}^{M} \alpha_i = 1. \tag{5}$$

Focusing on the extremal properties of z amounts then to considering the following one-dimensional contraction of Eq. (3):

$$\begin{aligned} F_n(u) = &\int_{a_1}^{b_1} dx_1 \cdots \int_{a_M}^{b_M} \rho(x_1, \ldots, x_M) \\ &\times \prod_{m=1}^{n-1} \theta\left(u - \sum_i \alpha_i x_i\right) \\ &\cdots \theta\left(u - \Phi^{(m)}\left(\sum_i \alpha_i x_i\right)\right) \end{aligned} \tag{6}$$

As a corollary, the invariant probability density $\rho(z)$ of z is obtained by differentiating the limiting form of (6) for $n = 1$,

$$\rho(z) = \int_{a_1}^{b_1} dx_1 \cdots \int_{a_M}^{b_M} \rho(x_1, \ldots, x_M) \delta\left(z - \sum_i \alpha_i x_i\right). \tag{7}$$

Notice that in systems involving a single variable x like, e.g., iterative mappings in the interval, z is identical to the variable in question, and Eq. (3) reduces to Eq. (6).

In this paper we are interested in the case where the dynamics is sufficiently complex to confer to the system nontrivial ergodic properties associated, e.g., to quasiperiodic or to chaotic behaviors. If as it happens typically the variables x_i and z_α possess nontrivial projections into the local unstable, stable, and neutral manifolds, then they will be locally subjected continuously to expansions, contractions, and reinjections. The question to be raised is, then, what is the signature of these processes on the extreme value properties, in the presence of several coupled variables. At the level of the multivariate cumulative distribution (3) one might suspect that, owing to the presence of the step functions, singularities will subsist along some phase space manifolds. On the other hand, at the level of the one-dimensional view afforded by Eq. (6) one expects that integration over all but one privileged degree of freedom will lead to smoothing, like, e.g., simple or higher order differentiability. If the monitored variable is the one subjected to such a smoothing, then one may wonder whether there still are some variables that bear the marks of dynamical complexity on extreme values and, if so, how to access them starting from the full set of original variables. These questions will be addressed in the subsequent sections.

III. FULLY DEVELOPED CHAOS IN DISCRETE-TIME LOW-DIMENSIONAL SYSTEMS

In order to sort out as directly as possible the new features arising from the coexistence of stable and unstable manifolds and of the reinjection of trajectories, we consider in this section the class of K flows, which are highly unstable dynamical systems in which each phase space point lies at the intersection of stable and unstable manifolds. A celebrated example of systems of this kind is the Baker transformation, defined in the phase space $0 \leqslant x \leqslant 1$, $0 \leqslant y \leqslant 1$ by the two-dimensional

mapping [6]:

$$\begin{aligned} x_1 &= 2x, \quad y_1 = \frac{y}{2} \quad 0 \leqslant x < \frac{1}{2}, \\ x_1 &= 2x-1, \quad y_1 = \frac{y+1}{2} \quad \frac{1}{2} \leqslant x \leqslant 1. \end{aligned} \tag{8}$$

Here x and y span thus, respectively, unstable and stable directions, and the part of the transformation defined by x in the right half of the unit interval is associated with the process of reinjection. This system possesses a positive and a negative Lyapunov exponent equal to $\sigma_1 = \ln 2$, $\sigma_2 = -\ln 2$ and a uniform invariant density $\rho(x,y) = 1$. Furthermore, projecting onto the x axis one obtains a closed evolution equation for x identical to the one-dimensional Bernoulli mapping. This closure property does not apply to the projection onto the y axis, since according to (8) the evolution of y is conditioned according to whether x is in the left or in the right part of the unit interval. In the sequel we evaluate successively the bivariate cumulative distribution $F_n(u,v)$ and its univariate contractions $F_n(u)$, $F_n(v)$ as well as the univariate cumulative distribution of a z-type variable [Eq. (5)] through which the roles of the stable and unstable manifolds become intertwined.

A. The bivariate cumulative distribution of extremes of the original variables and its one-dimensional contractions

Consider the first nontrivial case of window $n = 2$. Utilizing Eqs. (3) and (8) one obtains straightforwardly the following expressions.

(1) For $u < \frac{1}{2}$:

$$F_2(u,v) = \int_0^u dx \int_0^v dy \theta(u-2x)\theta\left(v - \frac{y}{2}\right).$$

Upon introducing the new variables $x' = 2x$, $y' = y/2$ and changing the integration limits accordingly, one arrives at

$$F_2(u,v) = \frac{uv}{2}. \tag{9a}$$

(2) For $u > \frac{1}{2}$:

$$\begin{aligned} F_2(u,v) = &\int_0^{\frac{1}{2}} dx \int_0^v dy \theta(u-2x)\theta\left(v-\frac{y}{2}\right) \\ &+ \int_{\frac{1}{2}}^u dx \int_0^v dy \theta(u-2x+1)\theta\left(v-\frac{y+1}{2}\right). \end{aligned}$$

The first integral can be handled as in the $u < 1/2$ case. The value of the second integral depends on whether v is smaller or larger than $1/2$. This yields

$$F_2(u,v) = \frac{uv}{2}, \quad u > \frac{1}{2}, \quad v < \frac{1}{2}, \tag{9b}$$

$$F_2(u,v) = \frac{uv}{2} + (2u-1)\left(v - \frac{1}{2}\right), \quad u > \frac{1}{2}, \quad v > \frac{1}{2}. \tag{9c}$$

To obtain the one-dimensional cumulative distributions of extremes for x and y we set, respectively, $v = 1$ and $u = 1$ in Eqs. (9). We obtain

$$\begin{aligned} F_2(u) &= \frac{u}{2}, \quad 0 \leqslant x \leqslant \frac{1}{2}, \\ &= \frac{3u-1}{2}, \quad \frac{1}{2} < x \leqslant 1, \end{aligned} \tag{10}$$

and

$$\begin{aligned} F_2(v) &= \frac{v}{2}, \quad 0 \leqslant y \leqslant \frac{1}{2}, \\ &= \frac{3v-1}{2}, \quad \frac{1}{2} < y \leqslant 1. \end{aligned} \tag{11}$$

We conclude that $F_2(u)$ and $F_2(v)$ are nondifferentiable at $u = 1/2$ and $v = 1/2$, and $F_2(u,v)$ is nondifferentiable along the manifold delimiting the upper right fourth of the unit square. The corresponding densities, $\rho_2(u) = dF_2/du$, $\rho_2(v) = dF_2/dv$ and $\rho_2(u,v) = \partial^2 F_2(u,v)/\partial u \partial v$, possess discontinuities on the corresponding values,

$$\begin{aligned} \rho_2(u) &= \tfrac{1}{2}, \quad 0 \leqslant u \leqslant \tfrac{1}{2}, \\ &= \tfrac{3}{2}, \quad \tfrac{1}{2} < u \leqslant 1, \end{aligned} \tag{12a}$$

$$\begin{aligned} \rho_2(v) &= \tfrac{1}{2}, \quad 0 \leqslant v \leqslant \tfrac{1}{2}, \\ &= \tfrac{3}{2}, \quad \tfrac{1}{2} < v \leqslant 1, \end{aligned} \tag{12b}$$

$$\begin{aligned} \rho_2(u,v) = \tfrac{1}{2}, &\quad 0 \leqslant u \leqslant \tfrac{1}{2}, \quad 0 \leqslant v \leqslant 1 \quad \text{and} \quad \tfrac{1}{2} < u \leqslant 1, \\ &0 \leqslant v \leqslant \tfrac{1}{2}, \\ = \tfrac{5}{2}, &\quad \tfrac{1}{2} < u \leqslant 1, \quad \tfrac{1}{2} < v \leqslant 1. \end{aligned} \tag{12c}$$

These results are in full agreement with the numerical evaluation of the different F_2 and ρ_2 starting from a time series of x and y generated by the Baker map. They are also in the same direction as previous results by the present authors [2,3], owing to the fact that x samples the dynamics along the unstable manifold and integrates therefore in an explicit way the role of the dynamical complexity in the properties of the extremes.

For reference, if x and y were independent uniformly distributed random variables in the unit interval, the statistical theory of extremes would lead to the quite different expressions

$$\begin{aligned} F_2(u,v) = u^2v^2, \quad \rho_2(u,v) = 4uv, \quad F_2(u) = u^2, \\ \rho_2(u) = 2u, \quad F_2(v) = v^2, \quad \rho_2(v) = 2v, \end{aligned} \tag{13}$$

all of which are smooth differentiable and monotonic functions of their arguments.

B. The cumulative distribution of extremes of a linear combination of the original variables

We next turn to the extreme value properties of a variable of the type of Eq. (5), which for the Baker map amounts to sampling the combined effect of the stable and unstable manifolds. For illustrative purposes we carry out the calculation in some detail for the case of $\alpha_1 = \alpha_2 = 1/2$, i.e., $z = (x+y)/2$.

We first evaluate the invariant density of z [Eq. (7)]:

$$\rho(z) = \int_0^1 dx \int_0^1 dy\, \delta\left(z - \frac{x+y}{2}\right),$$

or, introducing the variables $x' = x/2$, $y' = y/2$,

$$\rho(z) = 4\int_0^{\frac{1}{2}} dx'\theta(z-x')\theta\left(\frac{1}{2}-z+x'\right).$$

Using the constraints introduced by the step functions one obtains

$$\begin{aligned}\rho(z) &= 4z, \quad z < \tfrac{1}{2},\\ &= 4(1-z), \quad z > \tfrac{1}{2},\end{aligned} \tag{14}$$

which is to be contrasted with the uniform invariant density of the original variables.

Consider now the distribution of extremes for window $n = 2$. Using Eqs. (6) and (8) one has

$$\begin{aligned}F_2 = &\int_0^{\frac{1}{2}} dx \int_0^1 dy\, \theta\left(u-\frac{x+y}{2}\right)\theta\left(u-\frac{2x+\frac{y}{2}}{2}\right)\\ &+\int_{\frac{1}{2}}^1 dx \int_0^1 dy\, \theta\left(u-\frac{x+y}{2}\right)\theta\left(u-\frac{2x-1+\frac{y+1}{2}}{2}\right).\end{aligned} \tag{15}$$

Actually it is more informative to evaluate the density $\rho_2(u)$ associated to F_2, $\rho_2(u) = dF_2(u)/du$. This quantity is the sum of four terms in each of which one of the step functions appearing in Eq. (15) is replaced by a delta function. Introducing the same change of variables as in the calculation leading to Eq. (14), performing the delta function and evaluating the remaining parts by introducing the constraints imposed by the Heaviside function one arrives after a rather laborious calculation to the result

$$\begin{aligned}\rho_2(u) &= \frac{8u}{3}, \quad 0 \leqslant u \leqslant \frac{1}{4},\\ &= \frac{16u-2}{3}, \quad \frac{1}{4} < u \leqslant \frac{1}{2},\\ &= \frac{10-8u}{3}, \quad \frac{1}{2} < u \leqslant \frac{3}{4},\\ &= \frac{16(1-u)}{3}, \quad \frac{3}{4} < u \leqslant 1.\end{aligned} \tag{16}$$

Figures 1(a) and 1(b) depict this quantity along with the invariant density $\rho(z)$ associated to the monitored variable $(x+y)/2$. Both results are indistinguishable from those of a numerical evaluation starting from the time series of the original variables x and y. The point is that, contrary to the extreme value densities of the original variables displayed in Eqs. (12), the density of extreme values of the variable $z = (x+y)/2$ for window $n = 2$ possesses no discontinuity. Alternatively, the corresponding cumulative probability is now a (once-) differentiable function [Fig. 1(c)]. Clearly, this smoothing arises from the intertwining of the actions of the unstable and stable manifolds on the variable z, just as speculated in the end of Sec. II. Still, distribution (16) remains different from the distribution corresponding to the classical statistical theory, also depicted in Fig. 1(a) (dashed line):

$$\rho_{2,\mathrm{cl}}(u) = 4\int_0^1 dx \int_0^1 dy\, xy\, \delta\left(u-\frac{x+y}{2}\right).$$

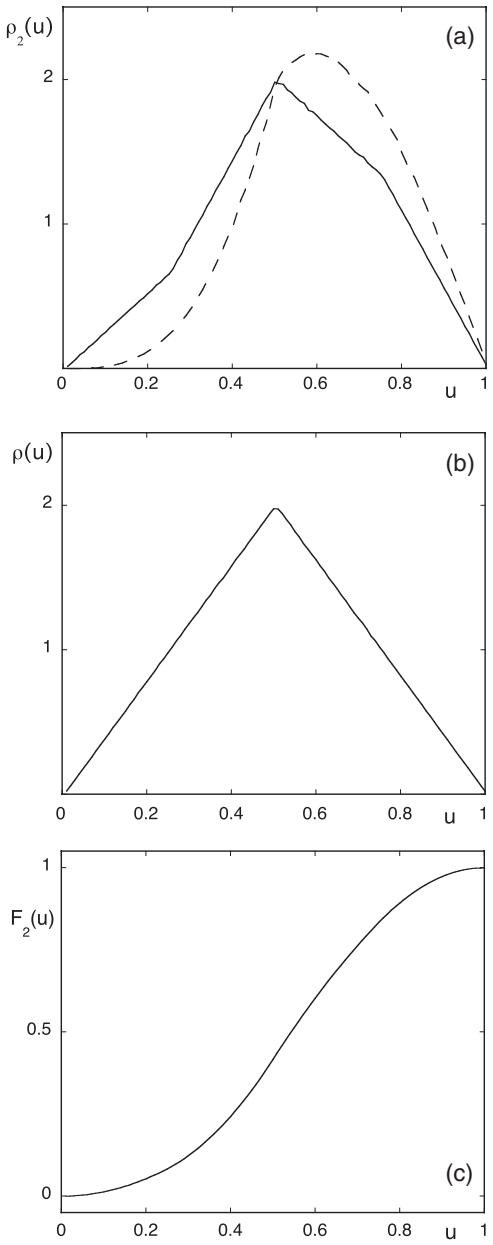

FIG. 1. Probability density of extremes associated to the variable $[\alpha_1 x + (1-\alpha_1)y]$ of system (8) with $\alpha_1 = 0.5$ and for a time window $n = 2$ (full line) (a); associated invariant probability density (b); and cumulative probability with $n = 2$ (c); as obtained analytically and numerically using 2×10^6 realizations. Dashed line in (a) stands for an i.i.d.r.v. process.

Notice that the invariant density of z in Fig. 1(b) is identical to that obtained from the classical statistical theory of i.i.d.r.v.'s.

Figures 2(a) and 2(b) depict the numerically evaluated $\rho_2(u)$ for two cases where the weights α corresponding to the x direction in expression (5) are $\alpha_1 = 0.05$ (or 0.95) and $\alpha_1 = 0.1$ (or 0.9). Again, the discontinuities in Eq. (12) are smoothed out, although the overall shape is less smooth than that of ρ_2 depicted in Fig. 1(a) for $\alpha_1 = 1/2$, being a succession of plateau-like parts joined by lines of high slopes. Furthermore, the number of points of nondifferentiability increases

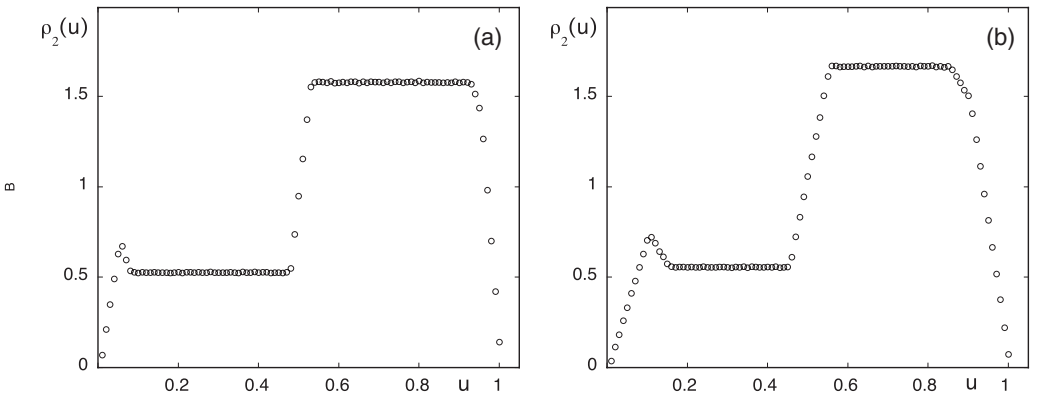

FIG. 2. As in Fig. 1(a) (full line) but for $\alpha_1 = 0.05$ (a); and $\alpha_1 = 0.1$(b); as obtained numerically.

with respect to Fig. 1(a). Analytic evaluations, though more involved, remain feasible. They are indistinguishable from the numerically obtained results and show that the discontinuities present in Eqs. (12) actually arise only in the limit $\alpha_1 = 0$ or $\alpha_1 = 1$: a mixing, however unbalanced, of the stable and unstable directions suffices to transform $\rho_2(u)$ from a discontinuous to a continuous nondifferentiable function. These trends persist in the case of observational windows larger than 2.

IV. CONTINUOUS-TIME LOW-DIMENSIONAL DYNAMICAL SYSTEMS

Typically, multivariate dynamical systems generating complex behavior are not of the K-flow type. Their evolution is, rather, a combination of unstable and stable motions, of stretchings, contractions, and foldings whose rates and phase space locations are distributed in a highly intricate way [4]. As a result the extreme value properties of a generic state variable are more likely to resemble those associated to Eq. (6), i.e., be smoother than those of variables borne by an unstable manifold or a trace thereof on a Poincaré surface of section. In this section we analyze the extreme value properties of this class of systems, focusing on continuous-time dynamical systems for which the deviations from K-type flows are the most marked. Furthermore, we limit ourselves to low-dimensional systems, where the detection of cross-over effects is easier.

A. The Lorenz model

We consider the classic Lorenz equations [7]:

$$\begin{aligned} \frac{dx}{dt} &= \sigma(-x + y), \\ \frac{dy}{dt} &= rx - y - xz, \\ \frac{dz}{dt} &= xy - bz. \end{aligned} \tag{17}$$

As is well known, for parameter values $\sigma = 10$, $b = 8/3$, and $r = 28$ Eqs. (17) generate a chaotic attractor. The trajectories on this attractor are organized to a large extent by the two-dimensional stable and the one-dimensional unstable manifolds of the trivial fixed point $x = y = z = 0$, and by the one-dimensional stable and the two-dimensional unstable manifolds of the two nontrivial fixed points $x_\pm = y_\pm = \pm\sqrt{b(r-1)}$, $z = r - 1$ [8]. As a result the model variables x, y, z are complex combinations of stable and unstable motions. Following the comments made in the previous section and the results summarized in Fig. 1(a) one is thus led to expect that their extreme value probabilistic properties should be free of some (if not all) of the singularities identified earlier as the principal signature of the deterministic character of the dynamics.

This expectation is confirmed by Fig. 3(a), showing the cumulative distribution of extremes u of the variable z for time windows 0.05 (dashed line) and 0.75 (full line) time units. The latter window is close to the mean time of switching of the trajectories in their spiral motion around (x_+, y_+, z) and (x_-, y_-, z). Both shapes are reminiscent of those of classical statistical theory.

Interestingly, under the same conditions the situation appears to be more involved as far as the extremes v of variable x is concerned, as depicted in Fig. 3(b). As can be seen, while F is practically smoothed out for window 0.05 it displays a more intricate, "nonclassical" structure for window 0.75. This suggests that to capture the role of the instability of motion in extreme value properties one needs to monitor an appropriate observable (here x, or y) sampled over time intervals of the order of the time where the effects of the instability show up through, e.g., the stretching and subsequent folding of the trajectories. Notice [Figs. 3(c) and 3(d)] that for window 0.75 the density of extrema of z appears smooth and unimodal, whereas that of x is bimodal and possesses a clearly distinguishable discontinuity for x values around zero.

As is well known, plotting in the Lorenz system the $n+1$st maximum of z versus the nth one gives rise to an everywhere unstable unimodal cusplike map possessing a smooth unimodal invariant density [Figs. 4(a) and 4(b)]. Figures 4(c) and 4(d) depict the cumulative probability of extremes u associated to this dynamical system and its corresponding density for window $n = 2$. We observe a very clear-cut signature of the underlying deterministic dynamics in the form of nondifferentiability of F_2 and discontinuity of ρ_2. The reason why the mapping of Fig. 4(a) captures this

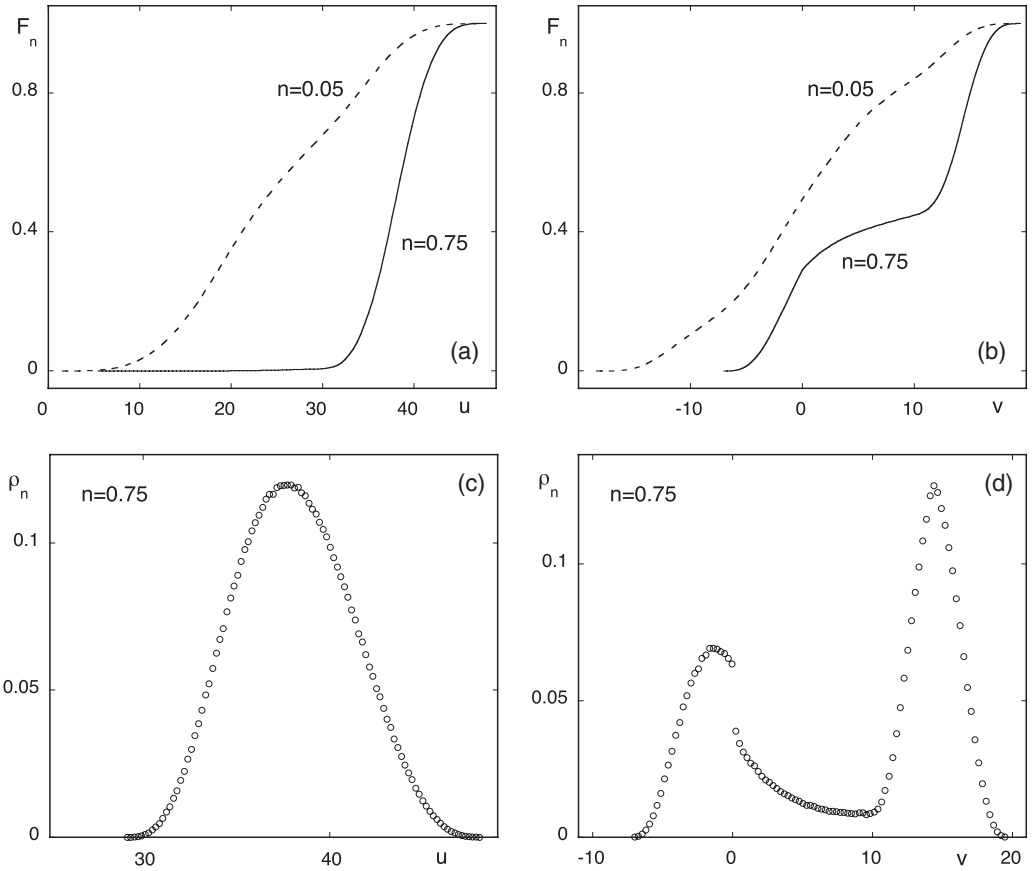

FIG. 3. (a)–(b) Cumulative distribution of extremes of variable z and x, respectively, associated to model (17) for time windows 0.05 and 0.75 time units. (c)–(d) Their associated probability densities as obtained numerically using 2×10^6 realizations.

phenomenon is similar to that concerning variable x in Fig. 3, namely, that the choice of time unit in the mapping, of the order of the mean time between the maxima of z, is such that the effects of the instability are allowed to show up in an explicit manner.

B. The Rössler model

The Rössler model [9]

$$\begin{aligned} \frac{dx}{dt} &= -y - z, \\ \frac{dy}{dt} &= x + ay, \\ \frac{dz}{dt} &= bx - cz + xz, \end{aligned} \tag{18}$$

for $a = 0.38$, $b = 0.30$, $c = 4.5$ provides a nice example of chaotic dynamics organized around a single fixed point (0, 0, 0). Linear stability analysis around this point leads to a pair of complex conjugate eigenvalues $\lambda_{1,2} \approx 0.15 \pm i0.98$ and a single real eigenvalue $\lambda_3 \approx -4.4$ of the Jacobian. These eigenvalues are associated to a two-dimensional unstable manifold close to the (x, y) plane and a one-dimensional stable one close to the z axis. Because of this, and in view of our previous results, one expects that the extreme value behavior of x and y will tend to be smoothed out more than that of z, which should be more intricate. This is confirmed by Fig. 5, where the cumulative distributions of extremes of the variables x and z are shown for a window of six time units. This window corresponds to the rightmost maximum of the probability density of reinjection times, which happens to be bimodal. Notice that for a small window, of, e.g., one or two time units, the behavior of both distributions is, at least qualitatively, close to the distributions of classical statistical theory (not shown). Figures 6(a) and 6(b) depict the probability densities corresponding to the distributions of Fig. 5. While they both present discontinuities those of $\rho_6(u)$ reflect the "nonclassical" feature that there is a substantial part of probability mass that remains in the region of values of z far from the upper bound of its domain of variation. This behavior arises from the intermittent character of the evolution of z (see also Ref. [2]), characterized by slow stages of gradual increase interrupted by rapid reinjections toward low values.

V. SPATIALLY EXTENDED SYSTEMS

The results reported in the preceding sections suggest that in a typical system comprising a large number of variables, the smoothing of the singularities of the extreme value properties, the signature of the complexity and of the deterministic character of the dynamics should become increasingly pronounced. In this section we address this point for a representative class of dynamical systems involving many variables, namely, spatially extended systems.

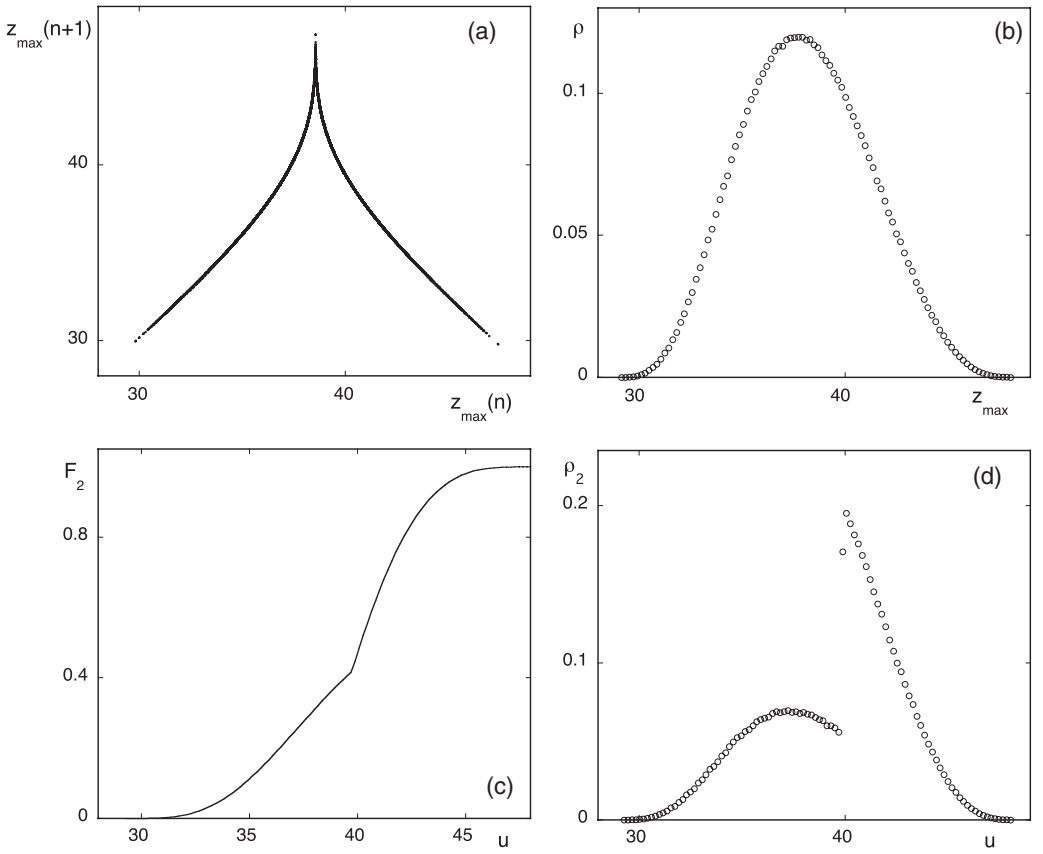

FIG. 4. Next amplitude plot of the maximum of variable z [Eqs. (17)] (a); associated invariant probability density (b); cumulative distribution of extremes (c); and probability density of extremes (d) for a time window $n = 2$ time units. Number of realizations as in Fig. 3.

Consider a discrete one-dimensional lattice of M spatially coupled elements each described by a continuous variable $x_n(j)$, where n is a discrete time and j is the lattice point. Let $f(x)$ be a function describing the local dynamics and D the coupling constant between a cell located on j with its first neighbors $j \pm 1$. The evolution of $x_n(j)$ is then given by the set of M coupled equations

$$x_{n+1}(j) = f(x_n(j)) + \frac{D}{2}[g(x_n(j+1)) + g(x_n(j-1)) - 2g(x_n(j))], \tag{19}$$

where g is the coupling function. In the sequel we will adopt the choice $g = f$ frequently made in the literature [10], choose an even number of cells and write Eqs. (19) as

$$x_{n+1}(j) = (1-D)f(x_n(j)) + \frac{D}{2}[f(x_n(j+1)) + f(x_n(j-1))], \quad 1 \leqslant j \leqslant M. \tag{20a}$$

Unless otherwise specified, periodic boundary conditions will be used throughout, and the domain of variation of x and $f(x)$ will be limited to the interval $[a,b]$,

$$x_n(j) = x_n(j+M), \qquad a \leqslant x \leqslant b, \qquad a \leqslant f(x) \leqslant b. \tag{20b}$$

Equations (20) are meant to be prototypical, encompassing large classes of dynamical systems giving rise to complex nonlinear behaviors. In this sense the function $f(x)$ describing the local dynamics is, typically, a one-dimensional endomorphism, as obtained by mapping an underlying continuous-time dynamics on a Poincaré surface of section and by subsequently projecting this mapping along the most unstable direction of the motion. The choice of nearest-neighbor coupling is

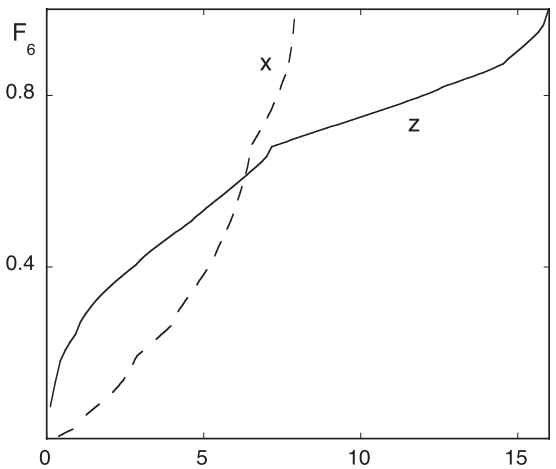

FIG. 5. Cumulative distribution of the extreme values of variables x and z [Eqs. (18)] for a time window of six time units. Number of realizations as in Fig. 3.

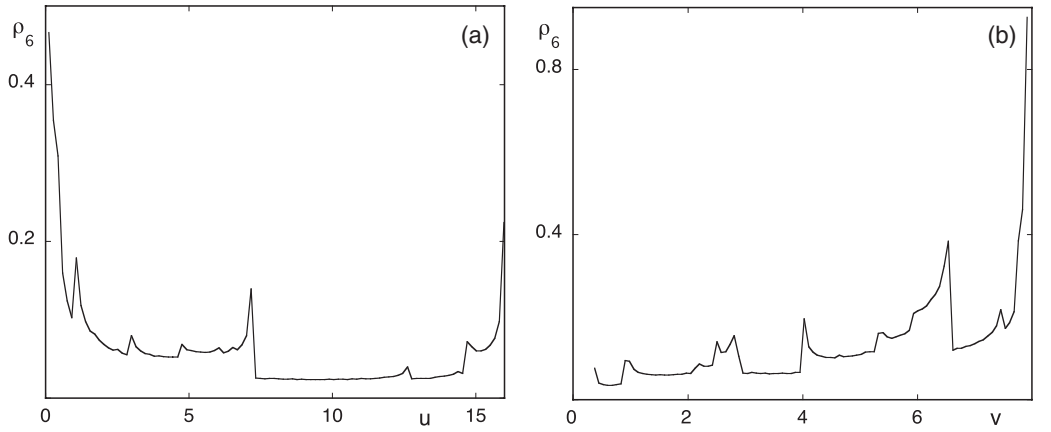

FIG. 6. As in Fig. 5 but for the probability density of extremes for variable z (a); and x (b).

motivated by the fact that most of the continuous time models representing real-world physico-chemical systems are in the form of partial differential equations involving the nabla or the Laplace operators, which, once discretized in space, couple any given point to its first neighbors only.

In spatially extended systems it is often useful to expand the variables in series of linearly independent functions incorporating symmetries and boundary conditions. Arguing in terms of the expansion coefficients, the modes, rather than the original variables, allows one then to capture collective properties that would otherwise remain blurred, especially if eventually the essence of the dynamics turned out to be borne by a limited number of modes. In view of the boundary conditions adopted a Fourier expansion appears to be the most

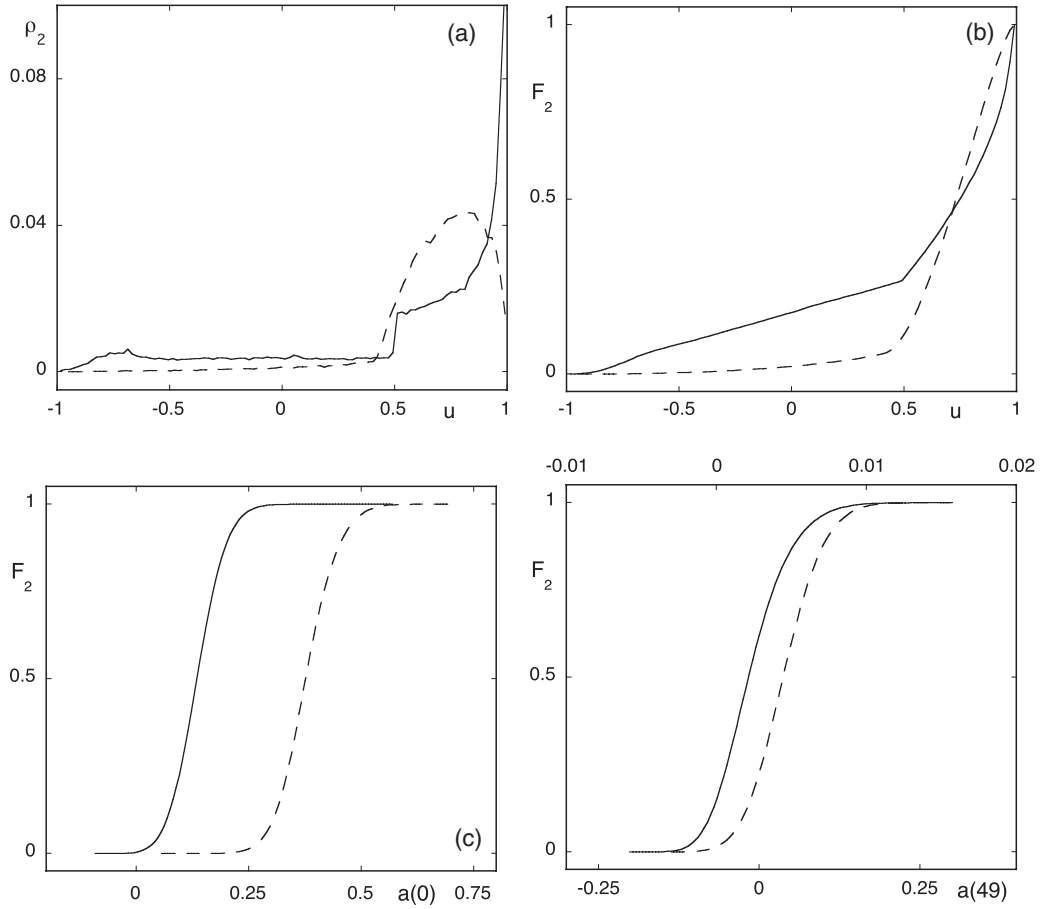

FIG. 7. Probability densities of extremes and their associated cumulative distributions as obtained from system (20) with $a = 2$, $M = 100$, $D = 0.01$ (full lines), $D = 0.4$ (dashed lines) and time window $n = 2$. (a)–(b) individual variable density and cumulative distributions. (c)–(d) Cumulative distributions of the slowest varying Fourier mode $a(0)$ and the fastest space varying one $a(49)$, respectively. Upper abscissa in (d) refers to the range of variation of $a(49)$. Number of realizations 10^5.

adequate one in this context,

$$a_n(k) = \frac{1}{M}\sum_{j=1}^{M}\left\{\cos\left(\frac{2\pi}{M}kj\right) + i\sin\left(\frac{2\pi}{M}kj\right)\right\}x_n(j), \quad k = 0,\ldots,M-1. \tag{21}$$

Among the different a_k, $a(0)$ and $a(M/2)$ are real and correspond to the space average and to the fastest space-varying combination of the $x(j)$, respectively,

$$a_n(0) = \frac{1}{M}\sum_j x_n(j),$$
$$a_n\left(\frac{M}{2}\right) = \frac{1}{M}\sum_j \cos(\pi j)x_n(j) = \frac{1}{M}\{-x(1)+x(2)-x(3)+\cdots\}, \tag{22}$$

All other modes are complex conjugate, with $a(k) = a^*(M-k)$. Notice that $a(0)$ and $a(M/2)$ are the only modes containing combinations of all the variables present.

In the following we analyze the extreme value properties of the original variables [Eqs. (20)] and of their Fourier modes [Eqs. (21)–(22)] for the representative case of coupled logistic maps,

$$f(x_n) = 1 - ax_n^2, \quad -1 \leqslant x_n \leqslant 1, \tag{23}$$

with $a = 2$ corresponding to the regime of fully developed chaos for the single map in the absence of spatial coupling. The state diagram of this system for $M = 100$ coupled maps has been investigated in detail by Kaneko [10]. He showed that for $a = 2$ and for a wide range of couplings D the behavior can be qualified as "fully developed turbulent" in the sense that it displays a pronounced local chaos with a rapid decay of spatial correlations, with the exception of a narrow band of coupling values where more ordered structures are observed. In what follows we inquire on the role of the coupling on the extreme value properties in the fully turbulent region.

The probability density of extremes for the first nontrivial window $n = 2$, $\rho_2(u)$ and its associated cumulative distribution $F_2(u)$ are depicted in Figs. 7(a) and 7(b) in the cases of weak ($D = 0.01$, full lines) and strong ($D = 0.4$, dashed lines) couplings. As can be seen the structure of the weak coupling case is quite fragmented and close to the fully discontinuous (for ρ_2) and nondifferentiable (for F_2) shapes arising in a single map in the absence of coupling. In contrast, in the strong coupling case both ρ_2 and F_2 appear quite smooth. As a matter of fact even for $D = 0.01$ there is no discontinuity in ρ_2 (and nondifferentiability in F_2) in the strict sense, the latter being the case only in the limit of the single map in the absence of coupling. We here have a situation analogous to that on Sec. III to the extent that a coupling, however weak, induces a number of negative Lyapunov exponents and hence the intertwining of unstable and stable manifolds.

In contrast to the foregoing the cumulative distribution of extremes associated to the Fourier modes $a(0)$ and $a(M/2)$ is smooth in both the weak and the strong coupling cases, as shown in Figs. 7(c) and 7(d). This behavior can be explained qualitatively by noticing that both modes can be viewed as sums of weakly correlated random variables and should therefore on these grounds be essentially controlled by the central limit theorem.

VI. CONCLUSIONS

Classical statistical approach enjoys a great popularity and success in a wide range of extreme value problems arising in nature, technology, and society. This is due to the fact that cumulative probability distributions of extremes as reconstituted from the observations seem to display sufficiently strong smoothness properties to be legitimately fitted by appropriate parametrizations of GEV-type distributions.

Real world systems involve as a rule a large number of variables and obey to deterministic evolution laws giving rise to complex behaviors. The guiding idea behind the present work has been twofold. First, that in the presence of several variables the effect of dynamical complexity on the probabilistic properties of extreme values tends to be masked by the intertwining between locally ongoing expansions, contractions, and reinjections in phase space. Second, that behind the apparent smoothness of the resulting probability distributions there exists an "organizing center" in the form of an appropriate combination of the variables probing the dominant unstable modes, which display singularities in, e.g., the form of nondifferentiability of the cumulative distributions of extremes on certain sets of phase space points. We have shown on a number of representative systems both analytically and by numerical simulations how these singularities are gradually smoothed out depending on the nature and on the number of variables involved. As it turns out smoothing is typically reflected by the regain of continuity on the probability density of extremes or of differentiability of the associated cumulative probability, but as a rule higher order singularities are bound to subsist.

In addition to their interest in the fundamental understanding of the origin of extreme value distributions in deterministic systems, our results have some potentially important applications. We suggest that smooth-looking extreme value distributions deduced from the data may actually contain higher order singularities inherited from their deterministic character and thus belong to a class of functions different from the GEV distributions. These differences should be more apparent for the probability distributions of certain privileged types of variables, and for not too long observational windows. Furthermore, quantities of operational interest for prediction purposes like, e.g., the return times of extremes [11] might prove to be more appropriate for revealing these differences. It would undoubtedly be interesting to conduct data analyses in this perspective and reassess the validity of some time-honored conclusions on the nature and the prediction of extreme events.

ACKNOWLEDGMENTS

This work is supported, in part, by the European Space Agency and the Belgian Federal Science Policy Office under contract numbers C90238 and C90241.

[1] P. Embrechts, P. Küppelberg, and T. Mikosch, *Modelling Extremal Events* (Springer, Berlin, 1999).
[2] V. Balakrishnan, C. Nicolis, and G. Nicolis, J. Stat. Phys. **80**, 307 (1995).
[3] C. Nicolis, V. Balakrishnan, and G. Nicolis, Phys. Rev. Lett. **97**, 210602 (2006).
[4] E. Ott, *Chaos in Dynamical Systems* (Cambridge University Press, Cambridge, 1993).
[5] R. L. Bras and I. Rodriguez-Iturbe, *Random Functions and Hydrology* (Dover, New York, 1985).
[6] V. Arnold and A. Avez, *Ergodic Problems of Classical Mechanics* (Benjamin, New York, 1968).
[7] E. N. Lorenz, J. Atmos. Sci. **20**, 130 (1963).
[8] C. Sparrow, *The Lorenz Equations* (Springer, Berlin, 1982).
[9] O. Rössler, Ann. N. Y. Acad. Sci. **316**, 376 (1979).
[10] K. Kaneko, Physica D **34**, 1 (1989).
[11] C. Nicolis and S. C. Nicolis, Europhys. Lett. **80**, 40003 (2007).